Functional Ecology

British Ecological Society

Functional Ecology 2012, **26**, 365–378 doi: 10.1111/j.1365-2435.2011.01954.x

Seasonal bryophyte productivity in the sub-Arctic: a comparison with vascular plants

Lorna E. Street[1,*,†], Paul C. Stoy[2], Martin Sommerkorn[3], Benjamin J. Fletcher[4], Victoria L. Sloan[4], Timothy C. Hill[1] and Mathew Williams[1]

[1]*School of Geosciences, University of Edinburgh, Edinburgh EH9 3JN, UK;* [2]*Department of Land Resources and Environmental Sciences, Montana State University, Bozeman, MT 59717, USA;* [3]*The James Hutton Institute, Craigiebuckler, Aberdeen AB15 8QH, UK; and* [4]*Department of Animal and Plant Sciences, University of Sheffield, Sheffield S10 2TN, UK*

Summary

1. Arctic ecosystems are experiencing rapid climate change, which could result in positive feedbacks on climate warming if ecosystem carbon (C) loss exceeds C uptake through plant growth. Bryophytes (mosses, liverworts and hornworts) are important components of Arctic vegetation, but are currently not well represented in terrestrial C models; in particular, seasonal patterns in bryophyte C metabolism compared to vascular plant vegetation are poorly understood.

2. Our objective was to quantify land-surface CO_2 fluxes for common sub-Arctic bryophyte patches (dominated by *Polytrichum piliferum* and *Sphagnum fuscum)* in spring (March–May) and during the summer growing season (June–August) and to develop a simple model of bryophyte gross primary productivity fluxes (P_B). We use the model to explore the key environmental controls over P_B for *P. piliferum* and *S. fuscum* and compare seasonal patterns of productivity with those of typical vascular plant communities at the same site.

3. The modelled total gross primary productivity (ΣP_B) over 1 year (March – November) for *P. piliferum* was *c.* 360 g C m^{-2} ground and for *S. fuscum c.* 112 g C m^{-2} ground, *c.* 90% and 30% of total gross primary productivity for typical vascular plant communities (ΣP_V) over the same year. In spring (March–May), when vascular plant leaves are not fully developed, ΣP_B for *P. piliferum* was $3 \times \Sigma P_V$.

4. Model sensitivity analysis indicated that bryophyte turf water content does not significantly affect (March–November) ΣP_B for *P. piliferum* and *S. fuscum*, at least for periods without sustained lack of precipitation. However, we find that seasonal changes in bryophyte photosynthetic capacity are important in determining ΣP_B for both bryophyte species.

5. Our study implies that models of C dynamics in the Arctic must include a bryophyte component if they are intended to predict the effects of changes in the timing of the growing season, or of changes in vegetation composition, on Arctic C balance.

Key-words: carbon, CO_2 flux, gross primary productivity, moss, photosynthesis, tundra, snow melt

Introduction

The Arctic climate is changing at a faster rate than the rest of the globe. Surface temperatures in the Arctic have increased at a rate of *c.* 0·4 °C per decade between 1966 and 2003 (McBean *et al.* 2005). If average annual global temperatures increase by 4 °C by the end of the century, large regions of the terrestrial Arctic are predicted to experience warming of 6 °C or more (Sanderson, Hemming & Betts 2011). Increases in Arctic surface temperature will be accompanied by shifts in ecosystem function, which could potentially result in the net release to the atmosphere of CH_4 or CO_2 from large stocks of organic C in northern permafrost soils; there is *c.* 98 Pg of C in North American Arctic soils alone (Ping *et al.* 2008). Increases in respiratory CO_2 flux that may result from warmer soils and melting permafrost may, however, be partially offset by enhanced plant productivity through greater availability of nutrients, and extension of the growing season (Schuur *et al.* 2009).

*Correspondence author. E-mail: l.e.street@sms.ed.ac.uk

Current understanding of photosynthesis in vascular plant canopies is well developed, with strong relationships demonstrated between vascular plant traits, such as leaf area, leaf N content and gross primary productivity (Shaver *et al.* 2007; Street *et al.* 2007; Williams *et al.* 2006). Bryophytes, however, are an important component of Arctic plant communities that have received relatively little research attention (but see, for example, Cornelissen *et al.* 2007; Douma *et al.* 2007). Existing estimates suggest that bryophytes account for a significant fraction of land-surface C uptake; bryophyte net primary productivity (NPP) accounts for around 25–30% of total above-ground NPP for Alaskan tussock tundra (Chapin *et al.* 1995), coastal tundra near Barrow (Miller *et al.* 1980) and Scandinavian tundra heath in the late summer (Campioli *et al.* 2009). Bryophytes can dominate photosynthetic CO_2 fluxes where they form a continuous cover (Douma *et al.* 2007) and can act as an important buffer against soil CO_2 losses to the atmosphere, assimilating as much as 51–98% of the daily respiratory CO_2 released from Siberian tundra soils (Sommerkorn, Bolter & Kappen 1999).

Bryophyte physiology differs from that of vascular plants with important consequences for land-atmosphere CO_2 fluxes. Bryophytes do not have stomata and lose water readily from their tissues (Proctor 2000), they also lack roots so are unable to extract water from depth within the soil profile. Bryophytes instead depend on the availability of water in the environment, from either humid air, the surface substrate or precipitation. Many species are adapted to survive long periods of desiccation. It follows that where bryophytes are a significant component of vegetation, the influence of external environmental conditions on photosynthesis will differ from that of vascular plant-dominated vegetation.

Recognition of the importance of bryophytes in the land-atmosphere exchange of CO_2 is growing (Huemmrich *et al.* 2010; Wania, Ross & Prentice 2009a,b), but the data supporting model representations are sparse. Much of the existing literature on Arctic bryophyte photosynthesis is based on laboratory measurements (Oechel & Collins 1976) or on field measurements on excised shoots where the natural structure of the bryophyte canopy had been disturbed (Harley *et al.* 1989; Murray *et al.* 1989). Few *in situ* CO_2 flux data are available on a per unit land-surface-area basis, and none cover the period during or immediately after snow melt (Douma *et al.* 2007; Miller *et al.* 1976; Oechel 1976; Sommerkorn, Bolter & Kappen 1999). Recent studies in the high Arctic that indicate the important bryophyte contribution to productivity (Arndal *et al.* 2009), especially after vascular plant senescence (Uchida *et al.* 2010), do not explicitly partition ecosystem CO_2 fluxes into bryophyte and vascular components.

In this study, we quantify land-atmosphere photosynthetic CO_2 fluxes (P_B) for two common Arctic bryophyte species, *Polytrichum piliferum* and *Sphagnum fuscum* (Fig. 1), and extrapolate measured *in situ* bryophyte fluxes (P_B) through time using simple models parameterised from laboratory observations. These models account for the influence of irradiance, bryophyte turf water content, snow cover and phenology on P_B. We also estimate vascular plant photosynthetic CO_2 fluxes (P_V) using a previously published model parameterised at the same sub-Arctic site at Abisko, Sweden. We combine measurements and models to address the following questions: (i) What are the controls over P_B in these species? and (ii) How does P_B compare to P_V across the growing season at the same site? We hypothesise that seasonal changes in photosynthetic capacity in bryophytes are less important than seasonal fluctuations in surface moisture content in controlling photosynthesis over the course of a year. We also expect that the relative contribution of P_B to be largest from March to May, the period during which the vascular plant canopy has yet to develop, but when moisture availability is high owing to snow melt, and when surface temperatures are above freezing. This study is the first to present *in situ* CO_2 flux data for bryophytes before the end of the snow season in the sub-Arctic.

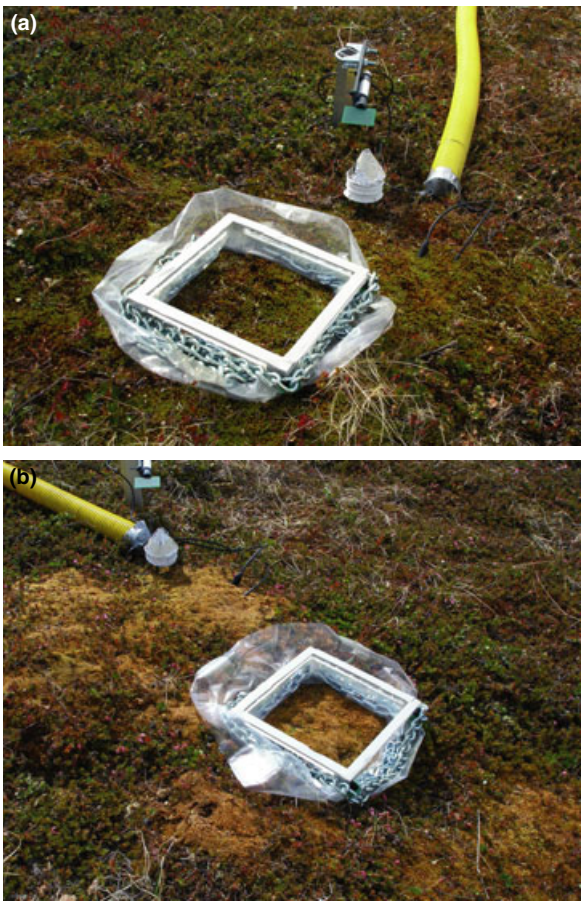

Fig. 1. Patches of (a) *Polytrichum piliferum* and (b) *Sphagnum fuscum* with chamber bases, surface moisture, temperature and volumetric water content (θ) sensors in place.

Materials and methods

FIELD MEASUREMENTS

Site description

Our field site was located near Abisko in northern Sweden, on a hillside *c.* 6 km south of Lake Torneträsk (68°18′N,18°51′E). Mean

annual temperature in the Abisko valley is −1 °C, mean July temperature is 11 °C, and annual precipitation averages *c*. 300 mm (Abisko Research Station, ANS). We chose to measure CO_2 flux on two common bryophyte species, both of which grow in continuous patches at the site: *Sphagnum fuscum* (Schimp.) H. Klinggr. forms hummocks in poorly drained areas, and *Polytrichum piliferum* Hedw. is locally abundant in rocky areas with thin organic soils (Fig. 1). The vascular vegetation at the site is dominated by ericaceous tundra heath composed of evergreen *Empetrum nigrum* L. (previously known as *Empetrum hermaphroditum* Hagerup), with dwarf shrubs *Betula nana* L. and *Salix spp*. in sheltered depressions, and barren cryptogam-dominated areas on exposed ridges.

Environmental conditions

Environmental conditions for *P. piliferum* and *S. fuscum* patches were monitored from June 2007 to August 2009 (at one flux plot for each species, Fig. 1). Bryophyte temperature was measured at 0·02 m depth below the surface (defined as the top of the moss mat), and air temperature, 0·03 m above the surface (with appropriate shielding from radiation) using HOBO 8-bit temperature sensors. Volumetric water content (θ, $m^3\ m^{-3}$) was measured for the top 0·01–0·05 m of bryophyte carpet using HOBO ECH_2O soil moisture probes (Onset Inc, Pocasset, MA, USA). Data were recorded every 5 min using HOBO Micro-Station data loggers (Onset Inc). We calibrated the soil moisture probes against destructive measurements of turf θ and calculated turf relative water content (u) as a percentage of dry mass. For details on the calibration procedure, see Appendix S1 in Supporting Information.

We measured light transmission through the snow pack on 2, 13, 15 and 20 April 2008. For details see Appendix S1.

Field CO_2 fluxes

We measured the net ecosystem exchange of CO_2 (F_c) (positive F_c representing a net flux from ecosystem to atmosphere) on three replicate bryophyte patches of *S. fuscum* and *P. piliferum* using a 0·2 × 0·2 × 0·13 m closed chamber system, on five dates from 21 June to 15 August 2007 and on 11 dates between 30 March and 25 April 2008. We selected which patches to measure based on continuous cover of each species on a level surface, to allow installation of the chamber bases. Methods followed Douma *et al*. (2007); for further details of the measurement protocol see Appendix S1. For each replicate plot, we made a series of F_c measurements under ambient and manipulated light conditions to create F_c light response curves. We first measured three replicates of F_c under ambient light conditions, followed by 4–7 measurements under sequentially reduced light conditions, created using layers of optically neutral shade cloth. We then

Table 1. List of symbols and units

Variable	Description	Units
θ	Volumetric water content	$m^3\ m^{-3}$
u	Relative water content	% dry mass
I	Irradiance	μmol photons $m^{-2}\ s^{-1}$
I_s	Irradiance under snow	μmol photons $m^{-2}\ s^{-1}$
P_B	Gross bryophyte photosynthetic CO_2 flux	μmol $CO_2\ m^{-2}\ s^{-1}$
ΣP_B	Total bryophyte gross primary productivity for specified period	g C m^{-2}
P_V	Gross vascular photosynthetic CO_2 flux	μmol $CO_2\ m^{-2}\ s^{-1}$
ΣP_V	Total gross vascular primary productivity for specified period	g C m^{-2}
F_c	Net ecosystem exchange	μmol $CO_2\ m^{-2}\ s^{-1}$
R_E	Ecosystem respiration	μmol $CO_2\ m^{-2}\ s^{-1}$
P_{max}	Theoretical light-saturated gross photosynthesis	μmol $CO_2\ m^{-2}\ s^{-1}$
K	Half-saturation constant of photosynthesis	μmol photons $m^{-2}\ s^{-1}$
P_{Tref}	P_{max} measured at the reference temperature	μmol $CO_2\ m^{-2}\ s^{-1}$
T	Temperature	K
T_{ref}	Reference temperature for photosynthesis	K
ΔS	Entropy term	J K^{-1} mol^{-1}
E_a	Activation energy	J mol^{-1}
E_d	Deactivation energy	J mol^{-1}
R	Gas constant	8·3143 J K^{-1} mol^{-1}
T_{opt}	Optimum temperature for photosynthesis	K
w_a	Parameter controlling response of photosynthesis to u	$(\%)^{-2}$
w_b	Parameter controlling response of photosynthesis to u	$(\%)^{-1}$
w_c	Parameter controlling response of photosynthesis to u	Dimensionless
τ	Light transmission through the snow pack	%
S	Snow depth	m
D	Day of year	Days
X_W	Adjustment factor for bryophyte relative water content	Dimensionless
X_D	Adjustment factor for day of year	Dimensionless
σ	Parameter representing photosynthetic capacity immediately after snow melt, relative to summer capacity	Dimensionless
D_{min}	Day of year at which increase in photosynthetic capacity commences	Days
D_{max}	Day of year at which maximum photosynthetic capacity is reached	Days
P_{maxL}	Light-saturated vascular photosynthesis per unit leaf area	μmol m^{-2} leaf s^{-1}
k	Beer's law extinction coefficient	Dimensionless
ε_0	Initial slope of the light response curve	μmol C μmol^{-1} photons

made three replicate measurements under fully darkened conditions to quantify ecosystem respiration (R_E). We subtracted F_c from mean R_E to calculate P_B.

During the spring 2008 measurement period, we followed the methods of Grogan & Jonasson (2006) and removed snow from the plots to measure CO_2 flux at the ground surface. We allowed at least 35 min post snow removal before making a measurement.

We also altered the measurement sequence, making additional measurements of R_E before decreasing the light level from ambient in stages, then re-measured respiration and repeated the sequence from ambient light back to zero (Fig. S1 in Supporting Information). We did this to detect any potential chamber effects on the background rate of R_E, a particular concern under cold conditions and after snow removal. Where possible, we took a small sample of bryophyte material to measure tissue u (for methods see Appendix S1), but did not take turf samples as the ground was frozen. In March–April 2008, we also made three measurements of ambient F_c, followed by three R_E measurements, on five replicate plots dominated by *E. nigrum* at the same site to assess photosynthetic activity. We used the 0·2 m × 0·2 m chamber and followed the same procedure as for the bryophyte flux measurements.

We calculated F_c from the rate of change in CO_2 concentration within the chamber (see Appendix S1) We then fitted rectangular hyperbola light response curves to the data using nonlinear least squares curve fitting in Matlab version 7.8.0 (MathWorks 2009):

$$P_B(I) = \frac{P_{max} I}{I + K} \quad \text{eqn 1}$$

where P_{max} is the rate of light-saturated photosynthesis and K is the half-saturation constant of photosynthesis. We used the fitted *in situ* P_B light response curves to adjust instantaneous *in situ* rates of P_B for differences in I between the instantaneous measurement and the half-hourly average I used to drive the model. Table 1 contains a list of symbols and units.

LABORATORY MEASUREMENTS

Photosynthesis response curves

We used laboratory-based CO_2 exchange measurements on samples of *P. piliferum* and *S. fuscum* to parameterise the bryophyte flux (P_B) model. We harvested *c.* 0·07 × 0·07 m turfs of *P. piliferum* and *S. fuscum* on 24 August 2007 and placed the turfs within controlled growth room facilities in the UK within 4 days. Conditions within the growth rooms were maintained at 12 °C with a 16/8-hour light/dark cycle until the beginning of November 2007. CO_2 flux measurements were made using a Walz gas analyser (Walz GmbH, Effeltrich, Germany) connected to a transparent 'mini-cuvette' in continuous differential mode. Turfs were trimmed to 0·04 × 0·04 m and placed within the cuvette. The CO_2 flux was allowed to stabilise for 2–3 min before a measurement was recorded. Light was supplied by two small halogen lamps, the intensity of which was adjusted using multiple sheets of optically neutral tissue paper placed over the cuvette. Air temperature, bryophyte turf temperature and light intensity were monitored inside the cuvette.

To quantify the response of photosynthesis to bryophyte turf water content, turfs of each species were fully wetted by soaking in distilled water. Net CO_2 fluxes (F_c) at I of 630 and 0 μmol m^{-2} s^{-1} were then measured at intervals as each turf dried evaporatively within the growth rooms, over 4 days. We measured the total weight of each turf before and after each flux measurement and subtracted F_c from the CO_2 flux at zero light (turf respiration) to calculate gross photosynthesis. We dried the *S. fuscum* sufficiently to observe a decrease in photosynthetic activity but did not allow the turfs to become fully desiccated (the minimum u for *S. fuscum* was 280% and *P. piliferum* was 65%, Fig. 5b). After the driest measurements, the turfs were re-wetted to optimal water content based on total turf weight. The turfs were allowed to recover in the growth rooms for at least 20 h, after which we measured the light response of P_B at 12 °C, then 5 °C and then 20 °C. The photosynthetic apparatus of both these moss types recovers quickly from desiccation, with full capacity reached within 24 h of re-wetting (from $u < 50\%$) for both *Polytrichum formosum* (Proctor, Ligrone & Duckett 2007) and *S. fuscum* (Hájek & Beckett 2008).

At each temperature, P_B measurements were made at I values of 500, 200, 100, 50, 1000 and then 0 μmol m^{-2} s^{-1}. During these measurements, the turfs were kept at water contents optimal for photosynthesis (on the basis of sample weight) by supplying small amounts of water to the base of the turf, and misting the top of each turf, after a measurement. After measurements were completed, we removed the green *P. piliferum* photosynthetic tissue and the *S. fuscum* capitula and weighed after drying at 70 °C for 3 days. There is very little photosynthetic activity below the capitulum region in *S. fuscum* (Street *et al.* 2011).

MODELLING

Bryophyte flux (P_B) model

The basic bryophyte flux (P_B) model consists of a rectangular hyperbola P_B response to irradiance (eqn 1), with the theoretical light-saturated rate of photosynthesis (P_{max}) varying as an Arrhenius function of temperature (eqns 2 and 3) (Warren & Dreyer 2006):
where

$$P_{max} = \frac{P_{T\mathrm{ref}} e^{\left[\frac{E_a}{RT_{\mathrm{ref}}} \times \left(1 - \frac{T_{\mathrm{ref}}}{T}\right)\right]}}{1 + e^{\left[\frac{\Delta_S T - E_d}{RT}\right]}} \left(1 + e^{\left(\frac{\Delta_S T_{\mathrm{ref}} - E_d}{RT_{\mathrm{ref}}}\right)}\right) \quad \text{eqn 2}$$

and where

$$\Delta_S = \frac{E_d}{T_{opt}} + R \ln\left(\frac{-E_a}{E_a - E_d}\right) \quad \text{eqn 3}$$

P_{max} is the theoretical light-saturated rate of photosynthesis, K is the half-saturation constant, $P_{T\mathrm{ref}}$ is P_{max} measured at the reference temperature T_{ref} (in this case 278 K), T is temperature, Δ_S is an entropy term, E_a is the activation energy, E_d is the deactivation energy, R is the gas constant, and T_{opt} is the temperature optimum for photosynthesis.

Modifications for bryophyte turf water content

To account for the effect of turf moisture content on P_B, we added a polynomial adjustment factor (X_w) to the basic P_B light–temperature model. X_w varied between 0 and 1, dependant on u:

$$P_B(I, u) = \frac{P_{max} I}{I + K} X_w \quad \text{eqn 4}$$

where

$$X_w = w_a u^2 + w_b u + w_c \quad \text{eqn 5}$$

where X_w is the water content adjustment factor and w_a, w_b and w_c are parameters.

Modifications for impact of snow on irradiance

To account for the impact of snow on light transmission to the bryophyte surface, we added a snow depth/*I* function that was parameterised in the field:

$$P_B(I,S) = \frac{P_{max} I_s}{I_s + K} \quad \text{eqn 6}$$

Where:

$$I_s = \begin{cases} I; & \text{if } S = 0\,\text{m} \\ I \times \tau; & \text{if } 0\,\text{m} < S < 0.03\,\text{m} \\ 0; & \text{if } S > 0.03\,\text{m} \end{cases} \quad \text{eqn 7}$$

Where I_s is estimated irradiance under snow, I is incident radiation, τ is light transmission through the snow pack, and S is snow depth.

We did not have continuous direct observations of snow cover over the plots, and albedo and snow depth measurements at a nearby eddy covariance station cannot account for the heterogeneous pattern of melt across the tundra landscape. We instead used measurements of air temperature at 0·03 m (one sensor located above one flux plot for each species) and 1·5 m above the surface (at meteorological station 50 m away) to estimate the presence or absence of snow over the plots for each species. For each day of the year (D), we assumed that the temperature sensors at 0·03 m were covered by snow, and the snow depth was therefore > 0·03 m, if and only if (i) the daily maximum air temperature at 1 m was > 0 °C, but the 0·03 m maximum air temp was ≤0 °C) or (ii) the amplitude of daily air temperature fluctuations was greater at 1·5 m than at 0·03 m. Otherwise, we assumed snow depth was < 0·03 m. After the final predicted snow day of each winter, we assumed all snow had melted from the plots once the minimum daily air temperature at 0·03 m > 1 °C. If snow depth was > 0·03 m, the irradiance under snow was assumed to be 0. If snow depth was < 0·03 m but > 0, we estimated irradiance under snow to be 40%, assuming 0·03 m snow depth. The transmission of light through the snow over time varies continuously as snow melts and accumulates. The effect of these assumptions on modelled P_B is described later in a formal uncertainty analysis.

Parameterising the P_B models

We parameterised the P_B model using laboratory flux data. For each sample, we fitted a light response curve (eqn 1) at each temperature (5, 12 and 20 °C). We then fitted the Arrhenius temperature response curves to the P_{max} values at each temperature (eqns 2 and 3). We estimated parameters E_a and E_d by assuming a P_B temperature optimum of 30 °C for each species following Longton (1988), who reported increasing *gross* photosynthesis up to 30 °C for *P. alpinum* at Barrow, Harley *et al.* (1989), who reported a temperature optimum for *S. fuscum* in Alaskan tussock tundra of > 30 °C, and Skre & Oechel (1981), who reported a temperature optimum for *S. fuscum* of > 25 °C in interior Alaskan taiga. To ensure that the fitted curve had a defined optimum (we did not measure at high enough temperatures to record temperature inhibition of photosynthesis and therefore constrain the Arrhenius function above 20 °C), we included an assumed zero point for photosynthesis at 65 °C when fitting the Arrhenius function. T_{ref} was 5 °C and P_{Tref} was the measured P_{max} for each sample at the reference temperature.

To calculate the parameters w_a, w_b and w_c, which define the shape of the P_B response to u, we used fitted values of K to calculate P_{max} for each of the turfs when measured during the drying experiment (during this part of the experiment, we measured P_B only at a constant I of 630 μmol m^{-2} s^{-1}). We then normalised the resulting P_{max} response curves by the maximum P_{max} for each turf and fitted eqn 5 for each sample. All curve fitting was carried out using nonlinear least squares in Matlab version 7.8.0 (MathWorks 2009).

We used the variability in fitted parameters across the five laboratory samples to represent natural variability between bryophyte patches within the model. We generated normal distributions for parameters E_a, E_d, K, w_a, w_b and w_c using the mean and standard deviation (SD) of fitted parameters from laboratory data. To account for covariance between parameters, we generated multivariate normal distributions based on the covariance matrices between the light and temperature response parameters (E_a, E_d, K and P_{Tref}) and between the parameters controlling the response to u (w_a, w_b and w_c). We then ran the model 300 times using random combinations of parameters drawn from these distributions. Modelled P_B is presented as the median, 10th and 90th percentile confidence interval (CI) of the 300 model runs.

Modifications for seasonal changes in photosynthetic capacity

Initial analysis using the $P_B(I,u)$ model configuration gave unrealistically high P_B in the spring (March–April) causing poor model fit (Table 3). We therefore included a further factor (X_D) to represent the seasonal development of bryophyte photosynthetic capacity between spring and summer:

$$P_B(I,D) = \frac{P_{max} I}{I + K} X_D \quad \text{eqn 8}$$

with

$$X_D = \begin{cases} \sigma & ; \text{if } 0 < D < D_{min} \\ \left(\frac{1-\sigma}{D_{max} - D_{min}}\right)(D - D_{min}) + \sigma & ; \text{if } D_{min} < D < D_{max} \\ 1 & ; \text{if } D_{max} < D < 365 \end{cases} \quad \text{eqn 9}$$

Where D_{min} is the day of year of onset of the increase in photosynthetic capacity (assumed to be the day after the last spring measurement, D = 115), D_{max} is the date at which the maximum capacity is reached (assumed to be the day before the first summer measurement, D = 172), and σ is a parameter representing relative photosynthetic capacity immediately after snow melt. We made a first approximation of the value of σ by calculating the ratio between the average P_{max} (for light curves where the maximum ambient I > 800 μmol m^{-2} s^{-1}) over the spring and summer measurement periods for each species (for *P. piliferum*, σ was 0·14; for *S. fuscum*, σ was 0·04). We assumed no decrease in photosynthetic capacity after the end of the summer season (Hicklenton & Oechel 1977). The impact of the values of σ, D_{min} and D_{max}, and alternative forms for eqn 9, are examined in detail in the section 'Bryophyte flux model sensitivity'.

Vascular photosynthesis model

We used the canopy photosynthesis model of Shaver *et al.* (2007) [hereafter referred to as the 'photosynthesis–light–irradiance' model

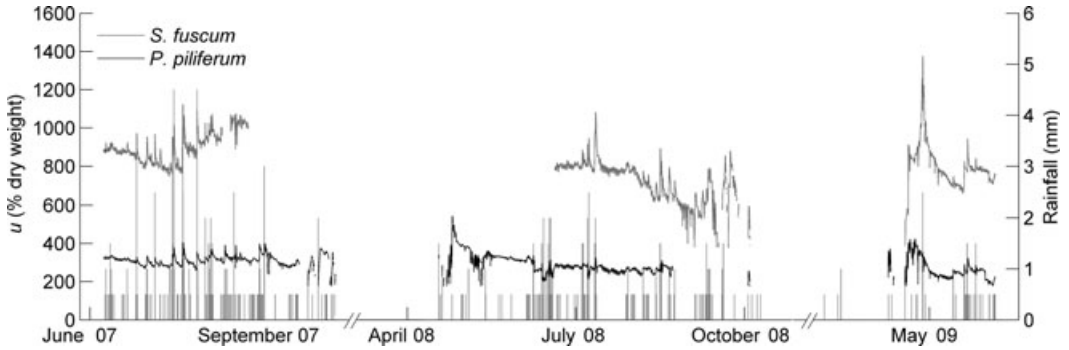

Fig. 2. Relative water content (u) of the *P. piliferum* and *S. fuscum* at the Abisko, Sweden, study site at 0·01–0·05 m depth. Data gaps occur when bryophyte surface temperature is below freezing (the probes do not function in frozen material) and for *S. fuscum* in early summer 2008 because of data logger malfunction. Vertical bars are half-hourly rainfall (mm).

or $P_V(L,I)$ model] to simulate P_V for heath vegetation (dominated by *Empetrum nigrum*) and dwarf birch (*Betula nana)*-dominated vegetation. Shaver *et al.* (2007) developed the model, which includes a respiration component, from 1 m × 1 m chamber net CO_2 flux data in tundra vegetation dominated by vascular plants. For *B. nana* and *E. nigrum*, the model was able to describe >85% of the variation in net CO_2 flux based on the leaf area, irradiance and temperature alone (Shaver *et al.* 2007). The photosynthesis component of the model [$P_V(L,I)$] is driven by two inputs, leaf area index of vascular plants (L) and irradiance (I):

$$P_V(L,I) = \frac{P_{\max L}}{k}\ln\left(\frac{P_{\max L} + \varepsilon_0 I}{P_{\max L} + \varepsilon_0 I e^{(-kL)}}\right) \quad \text{eqn 10}$$

where $P_{\max L}$ is the light-saturated photosynthetic rate per unit leaf area, k is the Beer's law extinction coefficient, and ε_0 is the initial slope of the light response curve. Model parameters for *B. nana*- and *E. nigrum*-dominated vegetation were taken from Table 7 of Shaver *et al.* (2007). We used the parameter standard deviations given in Shaver *et al.* (2007) to generate normal distributions of parameters and ran the model 300 times with random combination of these parameters to quantify model uncertainty.

For the 2008–2009 period, we drove the $P_V(L,I)$ model using a seasonal time series of L for both vascular species. To account for uncertainty in the estimate of seasonal L development, we synthesised measurements of L from several years at the same site and derive an upper and lower envelope for the L time course, based on the available data. We ran the $P_V(L,I)$ model for the upper and lower and mid-point estimates of L, assuming that the timing of leaf development was representative for 2008 and 2009. Details on the leaf area data used are given in Supplementary Information Appendix S1.

Throughout the analysis, the symbol Σ is used to represent a *total* photosynthetic C gain over a specified period, in g C m^{-2} (e.g. ΣP_B), as opposed to an instantaneous flux, in μmol m^{-2} s^{-1} (e.g. P_B).

Results

FIELD MEASUREMENTS

Environmental conditions

The relationship between θ and u differed significantly between the two species ($p < 0{\cdot}001$), reflecting that *S. fuscum* held more water per unit volume of turf than *P. piliferum* (Fig. S2). *In situ* minimum and maximum values of u during summer (June–August) 2008 were 200% and 340% for *P. piliferum*, and 620% and 1080% for *S. fuscum* (Fig. 2). There was an increase in the water content of the bryophyte surface during the snow melt period; for *P. piliferum*, u exceeded

Table 2. Plot descriptions with snow depths before snow removal (m) for 2008. Gaps in the table indicate that no flux measurements were made for that plot on that day. Relative water content (u) of bryophyte photosynthetic tissues is given in parentheses

		Snow depth (m) [u (% dry weight)]										
Plot	Species	31 March	02 April	03 April	10 April	11 April	12 April	13 April	15 April	20 April	22 April	25 April
1	*S. fuscum*	0·10						0	0·02			0
2	*S. fuscum*		0·12		0·12					0·11		
*3	*S. fuscum*			0·09						0·09		0·09
4	*P. piliferum*	0·025 (114)						0 (226)	0·01 (218)	0 (333)		0·005 (284)
*6	*P. piliferum*		0 (356)						0·01 (200)	0 (285)		0 (291)
7	*P. piliferum*		0·065		0·08							
27	*E. nigrum*					0						
41	*E. nig.* + *V. uli.*						0					
47	*E. nigrum*						0					
57	*E. nigrum*										0·01	
58	*E. nigrum*										0	

* indicates the location of HOBO micro-station loggers and sensors.
V. uli., *Vaccinium uliginosum*.

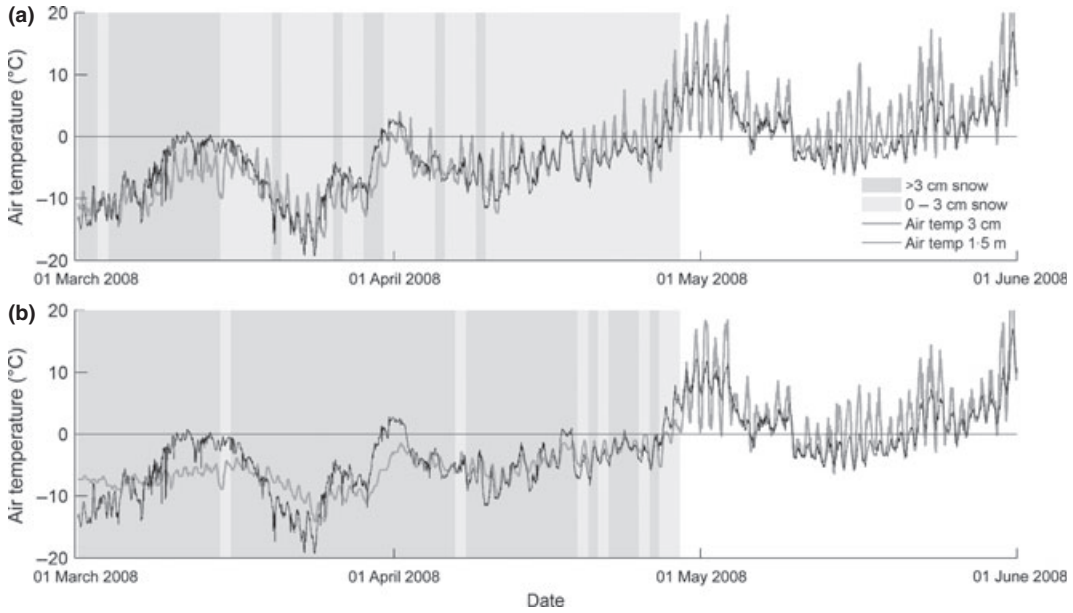

Fig. 3. Air temperature (°C) at 0·03 m for *P. piliferum* and *S. fuscum* and local air temperature at 1·5 m for March–May 2008 for (a) *P. piliferum* and (b) *S. fuscum*. Predicted snow cover days are shaded grey.

540% in April 2008, and for *S. fuscum*, *u* exceeded 1300% in April 2009 (Fig. 2). Values of *u* for *P. piliferum* (leaves only) during April 2008 measurement period were on average 256%, with a minimum of 114% on 31 March (Table 2).

Measured transmission of light through the snow pack was highly variable when the snow pack depth was $< 0{\cdot}05$ m. At 0·01 m depth, transmission varied between 20% and 80% of incoming radiation (Fig. S3). Using an exponential regression ($R^2 = 0{\cdot}64$), predicted transmission of light was 6% at 0·10 m depth and 42% at 0·03 m depth. On the basis of air temperature measurements, the predicted number of days where snow depth $> 0{\cdot}03$ m for the *P. piliferum* logger site was 18 for March–May 2008 and 27 for March–May 2009 (Fig. 3). The predicted number of snow days for the *S. fuscum* logger site was 51 for March–May 2008 and 48 for March–May 2009. Snow depth observations in 2008 were consistent with the predicted patterns of snow cover; on 25 April 2008, no snow was observed at the *P. piliferum* logger site, and 0·09 m of snow was present at the *S. fuscum* logger site (Table 2). The earliest predicted date of snow in 2008 was 29 October ($D = 302$), and the final date of snow melt for *P. piliferum* and *S. fuscum* was 29 April (Fig. 3).

Field CO_2 fluxes

Typical values of P_B for *P. piliferum* at ambient light levels were in excess of 4 μmol m^{-2} s^{-1} during June–August. P_B for *S. fuscum* was generally lower with typical values between 1 and 3 μmol m^{-2} s^{-1} (Figs 4a and 6a). Average light-saturated photosynthesis (P_{max}) during June–August for *P. piliferum* was $6{\cdot}5 \pm 0{\cdot}7$ μmol m^{-2} s^{-1} and for *S. fuscum* $2{\cdot}4 \pm 0{\cdot}3$ μmol m^{-2} s^{-1}. P_B for *P. piliferum* in April at ambient light levels was up to 0·5 μmol m^{-2} s^{-1} (Figs 4b and 6b), which corresponded to a net CO_2 uptake by the bryophyte

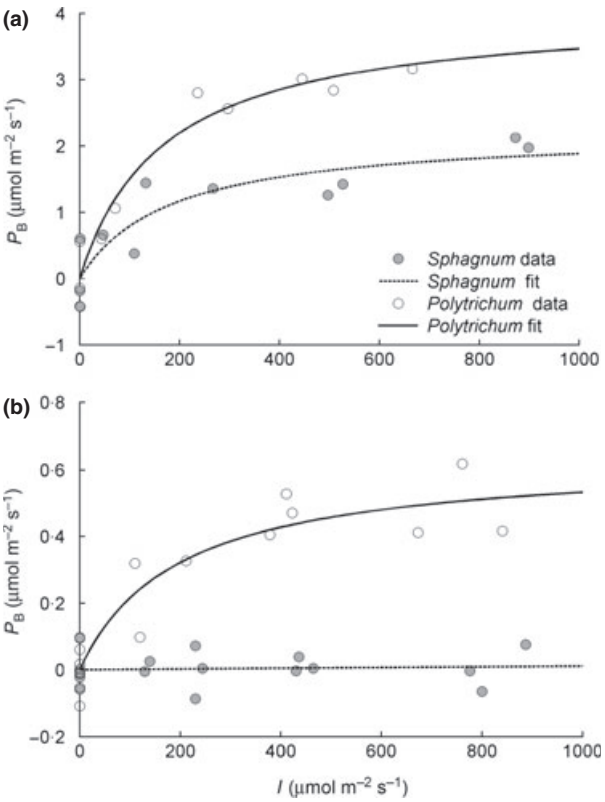

Fig. 4. Light response curves for gross primary productivity (P_B) in *P. piliferum* and *S. fuscum* in Abisko, Sweden, on (a) 15 August 2007 and (b) 25 April 2008. Note the difference in the *y*-axis scales.

surface of up to $-0{\cdot}3$ μmol m^{-2} s^{-1} (Fig. S1). For *S. fuscum*, P_B did not exceed 0·1 μmol m^{-2} s^{-1} in April (Fig. 6b). P_V for *E. nigrum* during March–April was not significantly different from zero ($-0{\cdot}01 \pm 0{\cdot}03$ μmol m^{-2} s^{-1}, data not shown). The

average variance of repeated R_E measurements (usually three) for light curves measured in June–August indicated an average measurement error variance of 0·26 μmol m^{-2} s^{-1}. During March–April, the average error variance on repeated measurements of R_E (usually between four and seven) for each light curve was 0·01 μmol m^{-2} s^{-1}. Measurements of R_E in the spring season before, during and after the light response curve indicated that the chamber effect on R_E over the course of the light curve was small (the average change in R_E was not significantly different from zero (*t*-test, $n = 16$, $P = 0{\cdot}11$), also see Fig. S1 for example light response curves plotted as time series).

LABORATORY MEASUREMENTS

Differences in photosynthetic activity between *P. piliferum* and *S. fuscum* in the field were also apparent in the laboratory data; *P. piliferum* had higher rates of gross photosynthesis. P_{max} at 20 °C for *P. piliferum* varied between 4·2 and 6·0 μmol m^{-2} s^{-1} and for *S. fuscum* between 1·0 and 3·2 μmol m^{-2} s^{-1} (Fig. 5a). The minimum and maximum fitted values of E_a and E_d for *P. piliferum* were 11 and 22 kJ mol^{-1} and 200 and 1302 kJ mol^{-1}. For *S. fuscum*, E_a was between 23 and 40 kJ mol^{-1} and E_d between 175 and 1230 kJ mol^{-1}. The fitted optimum turf *u* for photosynthesis was between 181% and 273% for *P. piliferum* and 185% and 701% for *S. fuscum* (Fig. 5b). The mean values of w_a, w_b and w_c for *P. piliferum* indicated that 90% photosynthetic capacity was reached when *u* was between 170% and 320 %, and for *S. fuscum*, 90% photosynthetic capacity was reached when *u* was between 390% and 800 %. Average photosynthetic tissue (green 'leaf') biomass for the *P. piliferum* flux samples was 193 ± 10 g m^{-2}, and capitulum biomass for *S. fuscum* was 211 ± 30 g m^{-2}.

MODELLING

The bryophyte flux model

Initial analysis that compared modelled P_B using $P_B(I,u)$, parameterised using laboratory data, against independent field measurements of P_B indicated that the model overestimated P_B during spring. The inclusion of X_D in $P_B(I,u,D)$, representing seasonal development of photosynthetic capacity, increased the R^2 of model vs. measured flux for *P. piliferum* from 0·49 to 0·79 and for *S. fuscum* from 0·62 to 0·76 (Table 3). Predicted ΣP_B for March–May decreased by more than two-thirds for both species as a result of including X_D. Inclusion of the adjustment factor for turf water content, X_W, did not improve the fit of the model (Table 3); we therefore did not include X_W in further analysis. The $P_B(I,D)$ model configuration, which accounted for seasonal increases in photosynthetic capacity, but no response to *u*, explained 81% of the variation in measured fluxes for *P. piliferum* and 81% for *S. fuscum*, with root mean square error (RMSE) of 1·0 and 0·49 μmol m^{-2} s^{-1} (Table 3 and Fig. 6).

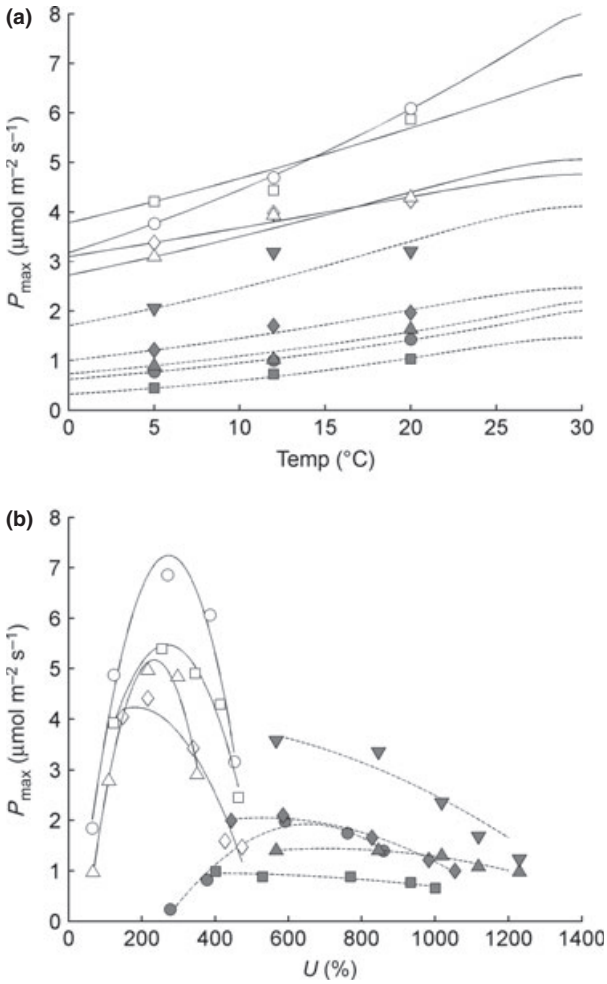

Fig. 5. Fitted light-saturated photosynthesis (P_{max}) for laboratory-measured *S. fuscum* and *P. piliferum* turfs in response to (a) temperature and (b) relative water content (*u*). Open symbols and solid lines represent *P. piliferum*, grey symbols and dashed lines represent *S. fuscum*, and different shaped symbols indicate different sample turfs.

Including the effect of snow in the model $P_B(I,D,S)$ had no significant impact on ΣP_B (Table 3), assuming negligible light transmission at snow depths > 0·03 m and 40% light transmission at snow depths < 0·03 m. The $P_B(I,D,S)$ model predicted total (March–November) ΣP_B for *P. piliferum* of 366 g C m^{-2} (10th–90th percentile CI of 308–434 g C m^{-2}) and for *S. fuscum* 111 g C m^{-2} (10th–90th percentile CI of 30–183 g C m^{-2}). For *P. piliferum*, ΣP_B during spring (March–May) was 20% of ΣP_B during summer (June-August). Spring season C uptake by *S. fuscum* was 13% of summer season uptake, assuming a linear increase in photosynthetic capacity between the end of April (*D* 115) and the 3rd week of June (*D* 172). Assuming no decline in photosynthetic capacity after the end of the summer season, ΣP_B for September-November was 36% of summer ΣP_B for *P. piliferum* and 34% for *S. fuscum* (Table 3).

The $P_V(L,I)$ model

Representative peak growing season *L* for *B. nana* vegetation was between 1·5 m^2 m^{-2} (Street *et al.* 2007) and 3·0 m^2 m^{-2}

Table 3. Root mean squared error (RMSE, in μmol m^{-2} s^{-1}) and r^2 for linear regressions of modelled vs. measured gross primary productivity (P_B) for different configurations of the P_B model. For each configuration, ΣP_B (g C m^{-2}) with 10th–90th percentile confidence interval is given for the spring season (March–May 2008 and 2009), summer season (June–August 2008) and autumn season (September–November 2008). *I* indicates that the model includes a light response; *D*, a day of year response; *u*, a water content response; and *S*, a snow depth response. ΣP_V for the same periods for *B. nana* and *E. nigrum* vegetation is calculated for maximum, mid and minimum *L* time series using the photosynthesis–leaf area–irradiance [$P_V(L,I)$] model.

				ΣP_B			
P_B model	Species	r^2	RMSE	March–May 08	June–August 08	September–November 08	March–May 09
$P_B(I,u)$	*P. piliferum*	0·49	2·0	131 (101–163)	234 (191–279)	84 (79–99)	147 (119–176)
	S. fuscum	0·62	0·8	41 (10–74)	73 (22–122)	24 (4–44)	39 (10–70)
$P_B(I,D,u)$	*P. piliferum*	0·79	1·1	40 (31–49)	228 (190–270)	84 (71–98)	46 (38–54)
	S. fuscum	0·76	0·6	10 (3–17)	72 (21·3–118)	26 (7–44)	9 (2–16)
$P_B(I,D)$	*P. piliferum*	0·81	1·0	46 (39–55)	238 (199–282)	85 (71–100)	48 (40–56)
	S. fuscum	0·81	0·5	9 (2–16)	73 (20–119)	25 (6–42)	9 (2–16)
$P_B(I,D,S)$	*P. piliferum*	–	–	46 (39–54)	235 (197–281)	85 (72–99)	47 (40–56)
	S. fuscum	–	–	10 (2–17)	76 (21–121)	26 (6–45)	10 (3–17)
				ΣP_V			
P_V model with	Species			March–May 08	Jun–Aug 08	September–November 08	March–May 09
Max *L*	*E. nigrum*			92 (86–97)	380 (345–419)	55 (51–59)	94 (89–100)
	B. nana			12 (11–13)	386 (339–434)	37 (34–40)	11 (10·8–11·9)
Mid *L*	*E. nigrum*			29 (27–31)	340 (309–369)	22 (21–23)	28 (26–29)
	B. nana			6 (6·0–6·5)	359 (328–392)	46 (43–49)	6 (5·7–6·2)
Min *L*	*E. nigrum*			0 (0–0)	263 (245–280)	0·14 (0·13–0·14)	0 (0–0)
	B. nana			0 (0–0)	295 (272–319)	0·19 (0·18–0·19)	0 (0–0)

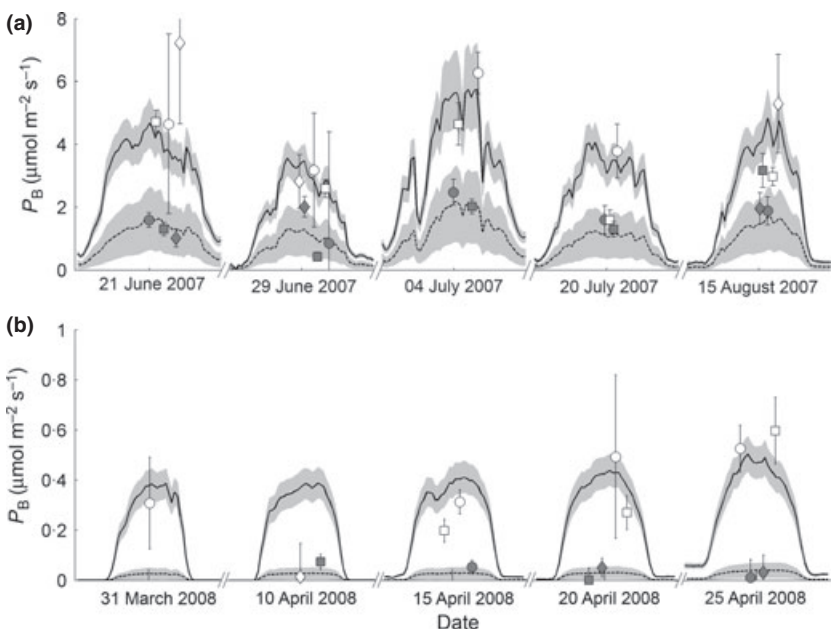

Fig. 6. Modelled and measured P_B (corrected for ambient light conditions) for (a) June–August 2007 and (b) March–April 2008. Open symbols and solid lines represent *P. piliferum*, grey symbols and dashed lines represent *S. fuscum*, and different shaped symbols indicate the three replicate plots. Errors bars are the 90% confidence interval for the P_B light response curve. Grey-shaded areas show the 10th–90th percentile of modelled P_B.

(Campioli 2008). *E. nigrum* peak season *L* was lower, between 1·25 (Street *et al.* 2007) and 2·0 m^2 m^{-2} (V. Sloan 2011) (Fig. 7). The $P_V(L,I)$ model predicts zero P_V when *L* is zero. The maximum *L* estimates gave a March–May ΣP_V estimate of 11 g C m^{-2} for *B. nana* and a 91 g C m^{-2} estimate for *E. nigrum*. Growing season estimates of ΣP_V for minimum and maximum *L* values were relatively more constrained, ranging from 263 to 380 g C m^{-2} for *E. nigrum* heath and 295 to 386 g C m^{-2} for *B. nana* communities (Table 3). Using the mid-point estimates of *L*, total (March-November) ΣP_V for *B. nana*-dominated vegetation was 411 g C m^{-2}, 2% of which occurred during spring

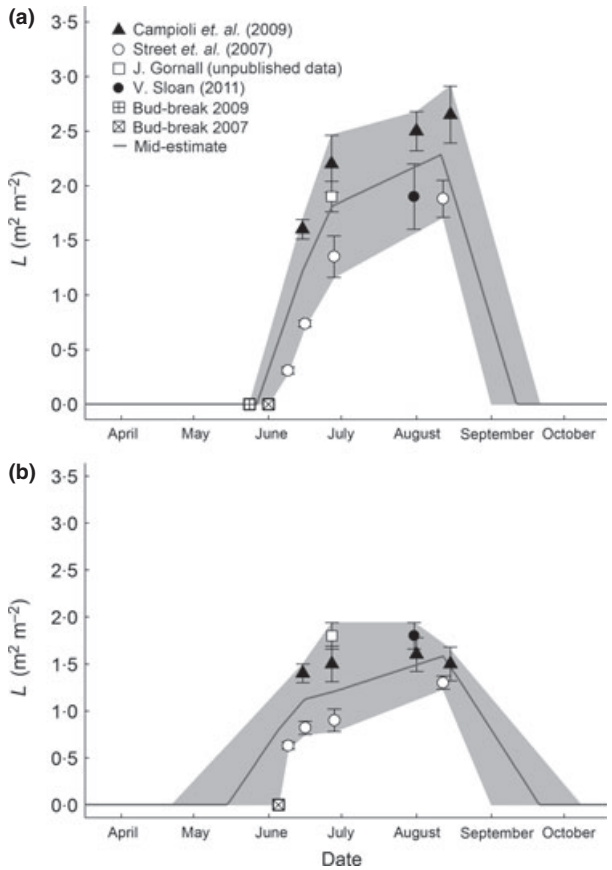

Fig. 7. Leaf area index (L) estimates used as input to the $P_V(L,I)$ model for (a) *B. nana* and (b) *E. nigrum* heath-dominated vegetation. The grey-shaded area shows the estimated L 'envelope' based on maximum and minimum values from available data sources. Closed symbols are based on destructive measurements of L, and open symbols are based on indirect estimates of L based on the normalised difference vegetation index (NDVI). Cross symbols show approximate observed dates of bud break at the same site.

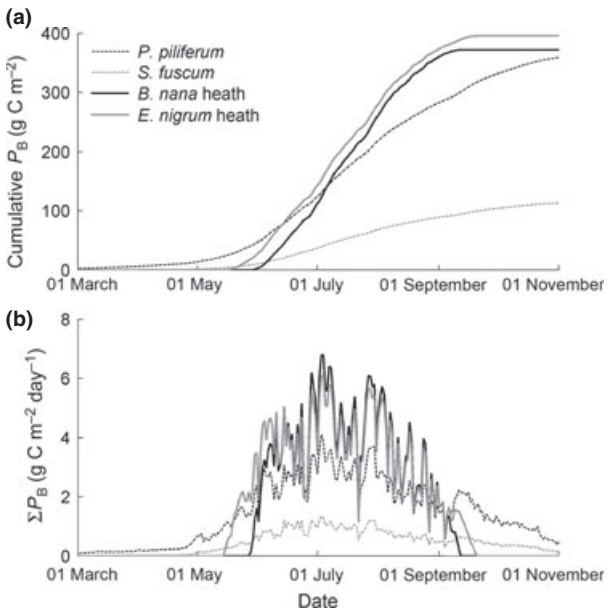

Fig. 8. (a) Cumulative modelled gross primary productivity (P_B, g C m^{-2}) and (b) daily ΣP_B (g C m^{-2} day^{-1}) for *P. piliferum*, *S. fuscum*, *B. nana* and *E. nigrum* heath vegetation for March–November 2008.

(March-May) and 11% during autumn (September-November). Total (March–November) ΣP_V for *E. nigrum*-dominated communities was 391 g C m^{-2}, 7% of which occurred during spring (March–May) and 6% during autumn (September-November, Table 3).

Comparing bryophyte and vascular productivity

Again assuming that L development followed the mid-point estimate, total (March–November) ΣP_B for *P. piliferum* was *c.* 90% and for *S. fuscum c.* 30% of shrub tundra vegetation (Table 3 and Fig. 8a). For *P. piliferum* in March–May, P_B was 160% of the P_V estimate for *E. nigrum* and 780 % for *B. nana* (assuming again the mid-point estimate of L). For *S. fuscum*, P_B in March–May was 33% of P_V for *E. nigrum* and 150% of P_V for *B. nana* (Table 3).

Bryophyte flux model sensitivity

We explored the sensitivity of the model outputs to both changes in major model assumptions (Table 4) and to one-dimensional perturbations in model parameters (Table 5).

Model assumptions

Photosynthesis at low temperatures. We assumed that the Arrhenius temperature response was applicable below 5 °C despite a lack of laboratory data or literature information on the response of gross photosynthesis to temperature below freezing. The Arrhenius fits, however, predicted photosynthetic activity at temperatures below literature values for the minimum temperature of physiological activity for *P. piliferum* and *S. fuscum*. We tested this model assumption by setting photosynthesis to zero below the minimum values for physiological activity of −7·5 °C for *P. piliferum* (Longton 1988) and −1 °C for *S. fuscum* (Gaberščik & Martinčič 1987). The effect of this model assumption on total spring P_B, however, was negligible (< 3 g C m^{-2}) (Table 4).

The time course of development of photosynthetic capacity. We assumed a linear increase in photosynthetic capacity between the end of the spring (March–May) measurement period and the beginning of the summer (June–August) measurement period. We test two alternative scenarios meant to represent end-members: (i) full photosynthetic capacity is reached 3 days after snow melt, $P_B(I,D,S)_{early}$, and (ii) full photosynthetic capacity is reached 3 days before the first summer measurement, $P_B(I,D,S)_{late}$. These scenarios significantly affect the spring (March–May) ΣP_B: the early scenario leads to an approximate doubling of ΣP_B

Table 4. Test of $P_B(I,D,S)$ model (P_B model incorporating response to light, day of year and snow depth) assumptions. ΣP_B (g C m^{-2}) is given for different configurations of the model for the spring (March–May), summer (June–August) and autumn (September–November), 2008. 10th–90th percentile confidence intervals are given in brackets.

Model	Description	Species	March–May 08	June–August 08	September–November 08
$P_B(I,D,S)$	$P_B(I,D,S)$ model without change	*P. piliferum*	46 (39–54)	235 (197–281)	84 (72–98)
		S. fuscum	10 (2–17)	76 (21–122)	26 (6–45)
$P_B(I,D,S)_{zero}$	Photosynthesis set to zero below −7·5 °C (*P. piliferum*) and −1 °C (*S. fuscum*)	*P. piliferum*	44 (38–51)	238 (199–279)	84 (71–97)
		S. fuscum	9 (2–16)	75 (23–125)	21 (6–36)
$P_B(I,D,S)_{early}$	Maximum photosynthetic capacity reached instantaneously 3 days after snow melt	*P. piliferum*	83 (71–96)	242 (202–285)	85 (72–98)
		S. fuscum	22 (7–36)	78 (27–123)	26 (8–44)
$P_B(I,D,S)_{late}$	Maximum photosynthetic capacity reached instantaneously 3 days before first summer measurement	*P. piliferum*	21 (17–24)	201 (168–237)	84 (70–98)
		S. fuscum	2 (0·4–3)	64 (18–102)	26 (6–44)
$P_B(I,D,S)_{trans}$	Transmission through > 0·03 m snow = 20%, through < 0·03 m snow = 100%	*P. piliferum*	46 (39–53)	234 (198–276)	84 (72–98)
		S. fuscum	10 (3–17)	78 (28–124)	27 (8–45)

Table 5. Sensitivity analysis for *P. piliferum* and *S. fuscum* parameterisations of the $P_B(I,D,S)$ model. Each row gives the root mean square error (RMSE) and r^2 for the linear regression of modelled vs. measured gross primary productivity (P_B), and the total P_B (mol C m^{-2}) for spring (March–May 2008 and 2009), summer (Jun–Aug 2008) and autumn (September–November 2008). Numbers in bold are for mean (nominal) parameters (in brackets after the parameter symbol). Single parameters were increased or decreased by 50% while other parameters were held at the nominal value

					ΣP_B		
Parameter	Units	Value	r^2	RMSE (μmol m^{-2} s^{-1})	March–May 08	June–August 08	September–November 08
P. piliferum (nominal)			0·81	1·03	44	218·2	81·8
E_a ($1·6 \times 10^4$)	J mol^{-1}	$2·3 \times 10^4$	0·79	1·04	43	235·9	80·7
		$7·8 \times 10^3$	0·81	1·18	45·3	202·4	83·3
E_d ($7·5 \times 10^5$)	J mol^{-1}	$1·1 \times 10^6$	0·81	1·03	44·3	218·2	81·8
		$3·7 \times 10^5$	0·81	1·03	44·3	218·2	81·8
K (107)	μmol m^{-2} s^{-1}	161	0·81	1·10	39·8	195·3	67·7
		54	0·80	1·01	51·2	252·8	108·9
P_{Tref} (3·6)	K	5·4	0·81	1·48	66·5	327·3	122·7
		1·8	0·81	1·95	22·2	109·1	40·9
S. fuscum (nominal)			0·81	0·45	12·8	78·6	25·5
E_a ($2·8 \times 10^4$)	J mol^{-1}	$4·2 \times 10^4$	0·78	0·49	12·1	90·4	24·0
		$1·4 \times 10^4$	0·81	0·59	13·8	68·8	27·4
E_d ($6·0 \times 10^5$)	J mol^{-1}	$9·0 \times 10^5$	0·81	0·45	12·8	78·6	25·5
		$3·0 \times 10^5$	0·81	0·45	12·8	78·5	25·5
K (77)	μmol m^{-2} s^{-1}	115	0·81	0·47	11·7	71·7	21·4
		38	0·81	0·43	14·5	88·7	33·3
P_{Tref} (1·1)	K	1·6	0·81	0·60	19·2	117·8	38·3
		0·5	0·81	0·85	6·4	39·3	12·8

for both species; the late scenario resulted in spring ΣP_B for *P. piliferum* of just 20 g C m^{-2} and for *S. fuscum* of 1·6 g C m^{-2} (Table 4).

Light transmission through snow. The $P_B(I,D,S)$ model assumes that either 0·03 m (40% light transmission), > 0·03 m (negligible light transmission) or 0 m snow (100% transmission) covered the bryophyte surface, based on air temperature measurements at the location of the flux plots. We tested the impact of this assumption by increasing the light transmission through > 0·03 m snow to 20%, and transmission through < 0·03 m to 100%. The effect on spring ΣP_B was negligible (< 1 g C m^{-2}) (Table 4).

Model parameters

We carried out a one-dimensional sensitivity analysis on the parameters of the $P_B(I,D,S)$ model by increasing or decreasing each parameter by 50% while keeping the other parameters constant (Table 5). The model was most sensitive to changing values of P_{Tref}. A 50% increase or decrease in P_{Tref} leads to a 50% increase or decrease in modelled ΣP_B and

RMSE. Model RMSE also increased with an increase in E_a, although seasonal ΣP_B was only slightly affected, with summer ΣP_B changing by < 10%. The model was relatively insensitive to changes in E_d or K (Table 5).

Discussion

THE MAGNITUDE OF BRYOPHYTE PRODUCTIVITY

Our results indicate that bryophytes can contribute substantially to cumulative Arctic land-surface carbon uptake. Total (April–November) ΣP_B for *P. piliferum* was *c.* 90% of ΣP_V for a deciduous shrub with peak season $L > 2$ m^2 m^{-2}. High rates of productivity per unit ground area for *P. piliferum* are consistent with previous studies on excised shoots (Oechel & Collins 1976; Penny & Bayfield 1982). While *S. fuscum* had lower rates of photosynthesis than *P. piliferum*, ΣP_B was still *c.* 30% of ΣP_V for shrub vegetation. The early onset of photosynthetic activity in bryophytes in spring, and delayed senescence in autumn, contributed to the large ΣP_B values. Our results are comparable with studies in northern spruce forests, which show that bryophytes can account for 10–50% of whole-forest gross CO_2 uptake (Goulden & Crill 1997).

P. piliferum occurs on scoured ridge tops often with little or no snow cover at the Abisko site. Where *P. piliferum* is present, photosynthetic C uptake can lead to net C gain by the ecosystem, *before* the snow pack melts across the wider landscape. Gross productivity for *P. piliferum* of up to 0·6 μmol m^{-2} m^{-1} during April exceeded rates for evergreen shrubs after snow removal (up to 0·26 μmol m^{-2} m^{-1}, Starr & Oberbauer (2003)). Rates of P_B for *S. fuscum* in April were much lower (< 0·1 μmol m^{-2} m^{-1}) perhaps because *S. fuscum* retains large amounts of water within capillary spaces which when frozen may restrict diffusion of CO_2 into tissues. The *S. fuscum* plots were less frequently without snow cover during April; this species grows in less well-drained, less exposed areas of the landscape.

CONTROLS OVER BRYOPHYTE CO_2 FLUX

We were unable to replicate the magnitude of P_B for *P. piliferum* in spring without including an increase in photosynthetic capacity between April and June. Depression of photosynthesis in spring was not because of low leaf water content (mean u was 260%), despite the bryophyte turf being frozen below leaf level. This was contrary to our expectation of finding no strong seasonal signal in P_B. The increase in photosynthetic activity during May and June could be the result of either: (i) increases in the biomass of photosynthetic tissues per m^2 ground through new growth; (ii) increased photosynthetic capacity as a result of increased allocation of resources to the photosynthetic apparatus (Williams & Flanagan 1998); or (iii) shifts in the temperature optimum for P_{max} (Oechel 1976; Sveinbjornsson & Oechel 1983), which we assumed to be constant throughout the season. Some bryophyte species do acclimate to ambient temperatures by shifting the temperature optimum for photosynthesis, for example, between early and late growing season, the temperature optimum for *net* photosynthesis for *Polytrichum alpinum* increased from *c.* 5 °C to 19 °C (Longton 1988), although this effect may be partly driven by temperature acclimation of respiration. As we measured the photosynthesis-temperature response after maintaining the mosses at a single temperature (12 °C), we could not parameterise a photosynthesis-temperature acclimation response in the model, but any increase in photosynthetic capacity because of temperature acclimation between spring and summer will be accounted for implicitly in the parameter σ.

Including the water content of the bryophyte turf did not improve the explanatory power of the model. This may be explained by (i) the relatively wet growing season of 2007, the longest period without at least 0·5 mm of precipitation between June and August was 4 days; (ii) the physiological adaptations of *P. piliferum* and *S. fuscum* to avoid drought conditions. For example, bryophytes of the genus *Polytrichum* are able to transport water from the substrate via internal conducting tissues and have some cuticular resistance to water loss (Thomas *et al.* 1996). *S. fuscum* is able to hold large amounts of water within tissues because of its dense growth form and the presence of hyaline cells and has a broad optimum water content for photosynthesis (Rydin & McDonald 1985). As a result, neither species experienced *in situ* turf water contents lower than the range over which P_{max} was 90 % of the optimum value. Turf water contents exceeded the upper limit of this range for both species, but any limiting effect on seasonal P_B totals was minor.

P_B MODEL SENSITIVITY

We identified the extent of light transmission through snow, the response of bryophyte photosynthesis to temperature at low temperature and the time course of seasonal development of photosynthetic capacity as major uncertainties in the model formulation. Exploration of the sensitivity of the model to these assumptions indicated that total P_B was most sensitive to the timing of changes in photosynthetic capacity between spring and summer. It is difficult to separate the effects of inadequate representation of the temperature response at low temperature, or potential shifts in the temperature optimum for photosynthesis, from the effect of increases in photosynthetic capacity. The *P. piliferum* plots, however, became visually greener between spring and summer, supporting our conclusion that photosynthetic capacity per unit ground area increased. These results suggest that future research should focus on phenological and physiological mechanisms underlying seasonality in photosynthesis for *P. piliferum*.

The parameters to which the model results were most sensitive were P_{Tref}, which controls the magnitude of photosynthetic activity, and E_a, which controls the shape of the P_{max} temperature response below the optimum temperature. Insensitivity of the model to E_d is unsurprising as this parameter controls the shape of the response curve above the optimum temperature, conditions that were infrequently

experienced in the field. The physiological activity of bryophyte tissue will also be affected by freeze/thaw cycles (Kennedy 1993). Including this effect in the P_B model would suppress photosynthetic C uptake following periods of extreme cold. While we take into account the presence of snow, we also did not include the effects of elevated CO_2 concentrations below the snow pack (Sommerkorn 2000), which could also act to increase rates of bryophyte photosynthesis.

SEASONALITY OF VASCULAR PHOTOSYNTHESIS

The size of the *L* envelope created from multiple data sources is a reflection of both inter-annual variability in the timing and extent of canopy development and spatial heterogeneity in *L*. The early and late season *L* for *B. nana* was well constrained by estimated dates of leaf bud burst and leaf fall, but there was large uncertainty in *L* for *E. nigrum* before and after the growing season. We treated *L* for the evergreen *E. nigrum* as a 'functional' leaf area, which we assumed was zero until the end of April as we did not observe photosynthesis before this date for *E. nigrum*. This is contrary to the findings of (Starr & Oberbauer 2003), but lack of measurable P_V may have been because of the much more exposed nature of the site. Our latest date for the onset of *E. nigrum L* development was set as the date of current year's leaf bud break (5 June 2009), but previous year's leaves will have been photosynthetically active before then (Street *et al.* 2007). Differences in ΣP_V for both species between maximum and minimum *L* estimates exceeded variability because of the parameter uncertainty reported by Shaver *et al.* (2007).

THE CONTRIBUTION OF BRYOPHYTES TO C EXCHANGE OF ARCTIC LANDSCAPES

Quantification of the total contribution of these bryophyte species to landscape-scale fluxes requires an estimate of abundance over the landscape and knowledge of landscape-level meteorology. Whereas *P. piliferum* is a highly productive species, its abundance as a fraction of the land surface is probably small, although potentially significant in exposed areas with low cover of vascular plants. The cover of *S. fuscum* as a proportion of ground area in tundra ecosystems is more significant, being frequently found in poorly drained areas. Other bryophyte species also contribute significantly to ground cover in these ecosystems; average total bryophyte cover over the Abisko tundra site is *c.* 45% (L. Street, unpublished data). Spadavecchia *et al.* (2008) quantified average peak season *L* over a 500 m × 500 m domain near to our study site to be 0·8 m^2 m^{-2}. This *L* approximates the lowest estimates of *L* for *B. nana* and *E. nigrum* used to drive the *P*(*L*,*I*) model. We might expect therefore that our lowest annual ΣP_V estimate (*c.* 260 g C m^{-2} $year^{-1}$) is a reasonable estimate for wider areas of the nearby tundra. As a first approximation, if all other moss species were equally productive as *S. fuscum* (at 100% cover, *c.* 110 g C m^{-2} $year^{-1}$), with cover of 45%, the total moss contribution to annual CO_2 flux over the wider landscape would be at least 20%. Different moss growth forms, however, may respond differently to environmental drivers, and annual C uptake may be restricted by periods of low tissue moisture (DeLucia *et al.* 2003). A reliable upscaling of moss productivity therefore requires more detailed information relating bryophyte growth form or water regulation strategy to landscape position.

We conclude that for *P. piliferum* and *S. fuscum*, seasonal changes in photosynthetic capacity are important in determining the magnitude of total gross CO_2 uptake, which can be comparable in magnitude to those of shrub tundra vegetation on a land-surface basis. Models of Arctic C dynamics must include a bryophyte component if they are intended to predict the effects of changes in vegetation composition, and of lengthening of the growing season, on C balance. The physiological response of bryophytes to low temperatures is a critical area for future research for the parameterisation of these models.

Acknowledgements

We would like to thank Katie Walker and Rachel Turton for their help with spring fieldwork, and ANS, Abisko for the provision of meteorological data and the invaluable support from their staff. We also thank Jonathan Evans at Centre for Ecology and Hydrology, Wallingford, UK, for providing access to field equipment. We thank Andrew Cole, Anne Goodenough and Rory O'Connor for help with summer fieldwork. R. Baxter and J. Gornall provided leaf area data. This study was supported by NERC PhD studentship to L. Street and the NERC-funded ABACUS project [University of Edinburgh and University of Sheffield (NE/D005884/1)].

References

Arndal, M.F., Illeris, L., Michelsen, A., Albert, K., Tamstorf, M. & Hansen, B.U. (2009) Seasonal variation in gross ecosystem production, plant biomass, and carbon and nitrogen pools in five high arctic vegetation types. *Arctic Antarctic and Alpine Research*, **41**, 164–173.

Campioli, M. (2008) *Carbon Allocation in Ecosystems: An Experimental and Modelling Approach for Tundra and Forest Vegetations*. Universiteit Gent, Gent.

Campioli, M., Samson, R., Michelsen, A., Jonasson, S., Baxter, R. & Lemeur, R. (2009) Nonvascular contribution to ecosystem NPP in a subarctic heath during early and late growing season. *Plant Ecology*, **202**, 41–53.

Chapin, F.S., Shaver, G.R., Giblin, A.E., Nadelhoffer, K.J. & Laundre, J.A. (1995) Responses of Arctic Tundra to experimental and observed changes in climate. *Ecology*, **76**, 694–711.

Cornelissen, J.H.C., Lang, S.I., Soudzilovskaia, N.A. & During, H.J. (2007) Comparative cryptogam ecology: a review of bryophyte and lichen traits that drive biogeochemistry. *Annals of Botany*, **99**, 987–1001.

DeLucia, E.H., Turnbull, M.H., Walcroft, A.S., Griffin, K.L., Tissue, D.T., Glenny, D., McSeveny, T.M. & Whitehead, D. (2003) The contribution of bryophytes to the carbon exchange for a temperate rainforest. *Global Change Biology*, **9**, 1158–1170.

Douma, J., van Wijk, M.T., Lang, S.I. & Shaver, G.R. (2007) The contribution of mosses to the carbon and water exchange of arctic ecosystems: quantification and relationships with system properties. *Plant, Cell and Environment*, **30**, 1205–1215.

Gaberščik, A. & Martinčič, A. (1987) Seasonal dynamics of net photosynthesis and productivity of *Sphagnum papillosum*. *Lindbergia*, **13**, 105–110.

Goulden, M.L. & Crill, P.M. (1997) Automated measurements of CO_2 exchange at the moss surface of a black spruce forest. *Tree Physiology*, **17**, 537–542.

Grogan, P. & Jonasson, S. (2006) Ecosystem CO_2 production during winter in a Swedish subarctic region: the relative importance of climate and vegetation type. *Global Change Biology*, **12**, 1479–1495.

Hájek, T. & Beckett, R.P. (2008) Effect of water content components on desiccation and recovery in *Sphagnum* Mosses. *Annals of Botany*, **101**, 165–173.

Harley, P.C., Tenhunen, J.D., Murray, K.J. & Beyers, J. (1989) Irradiance and temperature effects on photosynthesis of Tussock Tundra S. fuscum mosses from the foothills of the Philip Smith Mountains, Alaska. *Oecologia*, **79**, 251–259.

Hicklenton, P.R. & Oechel, W.C. (1977) Influence of light-intensity and temperature on field carbon-dioxide exchange of Dicranum-Fuscescens in Subarctic. *Arctic and Alpine Research*, **9**, 407–419.

Huemmrich, K.F., Gamon, J.A., Tweedie, C.E., Oberbauer, S.F., Kinoshita, G., Houston, S., Kuchy, A., Hollister, R.D., Kwon, H., Mano, M., Harazono, Y., Webber, P.J. & Oechel, W.C. (2010) Remote sensing of tundra gross ecosystem productivity and light use efficiency under varying temperature and moisture conditions. *Remote Sensing of Environment*, **114**, 481–489.

Kennedy, A.D. (1993) Photosynthetic response of the Antarctic Moss *P. piliferum*-Alpestre Hoppe to low-temperatures and freeze-thaw stress. *Polar Biology*, **13**, 271–279.

Longton, R.E. (1988) *Biology of Polar Bryophytes and Lichens*. Cambridge University Press, Cambridge.

MathWorks (2009) MATLAB version 7.8.0 MathWorks, Natick, Massachusetts, USA.

McBean, G., Alekseev, G., Chen, D., Førland, E., Fyfe, J., Groisman, P.Y., King, R., Melling, H., Vose, R. & Whitfield, P.H. (2005) Arctic climate: past and present. *Arctic Climate Impact Assessment: Scientific Report*. pp. 21–60, Cambridge University Press, Cambridge, UK.

Miller, P.C., Oechel, W.C., Stoner, W.A. & Sveinbjornsson, B. (1976) Simulation of CO_2 uptake and water relations of four Arctic bryophytes at point barrow, Alaska. *Photosynthetica*, **12**, 7–20.

Miller, P.C., Webber, P.J., Oechel, W.C. & Tieszen, L.L. (1980) Biophysical processes and primary production. *An Arctic Ecosystem: the Coastal Tundra at Barrow, Alaska* (eds J.M. Brown, P.C. Miller, L.L. Tieszen & F.L. Bunnell), pp. 66–101, Dowden, Hutchinson & Ross, Inc., Stroudsburg, PA.

Murray, K.J., Harley, P.C., Beyers, J., Walz, H. & Tenhunen, J.D. (1989) Water-content effects on photosynthetic response of *S. fuscum* Mosses from the foothills of the Philip Smith Mountains, Alaska. *Oecologia*, **79**, 244–250.

Oechel, W.C. (1976) Seasonal patterns of temperature response of CO_2 flux and acclimation in arctic Mosses growing *in Situ*. *Photosynthetica*, **10**, 447–456.

Oechel, W.C. & Collins, N.J. (1976) Comparative CO_2 exchange patterns in Mosses from 2 Tundra Habitats at Barrow, Alaska. *Canadian Journal of Botany-Revue Canadienne De Botanique*, **54**, 1355–1369.

Penny, M.G. & Bayfield, N.G. (1982) Photosynthesis in desiccated shoots of *P. piliferum*. *New Phytologist*, **91**, 637–645.

Ping, C.-L., Michaelson, G.J., Jorgenson, M.T., Kimble, J.M., Epstein, H., Romanovsky, V.E. & Walker, D.A. (2008) High stocks of soil organic carbon in the North American Arctic region. *Nature Geoscience*, **1**, 615–619.

Proctor, M.C.F. (2000) The bryophyte paradox: tolerance of desiccation, evasion of drought. *Plant Ecology*, **151**, 41–49.

Proctor, M.C.F., Ligrone, R. & Duckett, J.G. (2007) Desiccation tolerance in the Moss *Polytrichum formosum*: physiological and fine-structural changes during desiccation and recovery. *Annals of Botany*, **99**, 75–93.

Rydin, H. & McDonald, A.J.S. (1985) Tolerance of *S. fuscum* to water level. *Journal of Bryology*, **13**, 571–578.

Sanderson, M.G., Hemming, D.L. & Betts, R.A. (2011) Regional temperature and precipitation changes under high-end (> = 4 degrees C) global warming. *Philosophical Transactions of the Royal Society a-Mathematical Physical and Engineering Sciences*, **369**, 85–98.

Schuur, E.A.G., Vogel, J.G., Crummer, K.G., Lee, H., Sickman, J.O. & Osterkamp, T.E. (2009) The effect of permafrost thaw on old carbon release and net carbon exchange from tundra. *Nature*, **459**, 556–559.

Shaver, G.R., Street, L.E., Rastetter, E.B., Van Wijk, M.T. & Williams, M. (2007) Functional convergence in regulation of net CO2 flux in heterogeneous tundra landscapes in Alaska and Sweden. *Journal of Ecology*, **95**, 802–817.

Skre, O. & Oechel, W.C. (1981) Moss functioning in different Taiga ecosystems in interior Alaska. 1. Seasonal, phenotypic, and drought effects on photosynthesis and response patterns. *Oecologia*, **48**, 50–59.

Sloan, V. (2011) *Plant Roots in Arctic Ecosystems: Stocks and Dynamics and their Coupling to Aboveground Parameters*, PhD Thesis, pp. 31–50 & 88–93. University of Sheffield.

Sommerkorn, M. (2000) The ability of lichens to benefit from natural CO_2 enrichment under a spring snow-cover: a study with two arctic-alpine species from contrasting habitats. *Bibliotheca Lichenologica*, **75**, 365–380.

Sommerkorn, M., Bolter, M. & Kappen, L. (1999) Carbon dioxide fluxes of soils and mosses in wet tundra of Taimyr Peninsula, Siberia: controlling factors and contribution to net system fluxes. *Polar Research*, **18**, 253–260.

Spadavecchia, L., Williams, M., Bell, R., Stoy, P.C., Huntley, B. & van Wijk, M.T. (2008) Topographic controls on the leaf area index and plant functional type of a tundra ecosystem. *Journal of Ecology*, **96**, 1238–1251.

Starr, G. & Oberbauer, S.F. (2003) Photosynthesis of arctic evergreens under snow: Implications for tundra ecosystem carbon balance. *Ecology*, **84**, 1415–1420.

Street, L.E., Shaver, G.R., Williams, M. & Van Wijk, M.T. (2007) What is the relationship between changes in canopy leaf area and changes in photosynthetic CO2 flux in arctic ecosystems? *Journal of Ecology*, **95**, 139–150.

Street, L.E., Subke, J.A., Sommerkorn, M., Heinemeyer, A. & Williams, M. (2011) Turnover of recently assimilated carbon in arctic bryophytes. *Oecologia*, **167**, 325–337.

Sveinbjornsson, B. & Oechel, W.C. (1983) The effect of temperature preconditioning on the temperature sensitivity of net Co2 Flux in geographically diverse populations of the Moss *P. piliferum*-commune. *Ecology*, **64**, 1100–1108.

Thomas, R.J., Ryder, S.H., Gardner, M.I., Sheetz, J.P. & Nichipor, S.D. (1996) Photosynthetic function of leaf lamellae in *P. piliferum* commune. *Bryologist*, **99**, 6–11.

Uchida, M., Kishimoto, A., Muraoka, H., Nakatsubo, T., Kanda, H. & Koizumi, H. (2010) Seasonal shift in factors controlling net ecosystem production in a high Arctic terrestrial ecosystem. *Journal of Plant Research*, **123**, 79–85.

Wania, R., Ross, I. & Prentice, I.C. (2009a) Integrating peatlands and permafrost into a dynamic global vegetation model: 1. Evaluation and sensitivity of physical land surface processes. *Global Biogeochemical Cycles*, **23**, GB3014, doi:10.1029/2008GB003412.

Wania, R., Ross, I. & Prentice, I.C. (2009b) Integrating peatlands and permafrost into a dynamic global vegetation model: 2. Evaluation and sensitivity of vegetation and carbon cycle processes. *Global Biogeochemical Cycles*, **23**, GB3015, doi:10.1029/2008GB003413.

Warren, C.R. & Dreyer, E. (2006) Temperature response of photosynthesis and internal conductance to CO2: results from two independent approaches. *Journal of Experimental Botany*, **57**, 3057–3067.

Williams, T.G. & Flanagan, L.B. (1998) Measuring and modelling environmental influences on photosynthetic gas exchange in S. fuscum and Pleurozium. *Plant Cell And Environment*, **21**, 555–564.

Williams, M., Street, L.E., van Wijk, M.T. & Shaver, G.R. (2006) Identifying differences in carbon exchange among Arctic ecosystem types. *Ecosystems*, **9**, 288–304.

Received 28 June 2011; accepted 28 November 2011
Handling Editor: David Whitehead

Supporting information

Additional Supporting information may be found in the online version of this article.

Figure S1. Spring P_B light response curve measurement plotted as time series.

Figure S2. Calibration of ECH_2O soil moisture probes.

Figure S3. Measured extinction of light with snow depth.

Appendix S1. Methodological details.

As a service to our authors and readers, this journal provides supporting information supplied by the authors. Such materials may be re-organized for online delivery, but are not copy-edited or typeset. Technical support issues arising from supporting information (other than missing files) should be addressed to the authors.